Available online at www.sciencedirect.com
ScienceDirect
International Journal of Heat and Mass Transfer 50 (2007) 2060–2068
International Journal of HEAT and MASS TRANSFER
www.elsevier.com/locate/ijhmt

Inverse estimation of heat flux and temperature in multi-layer gun barrel

Tsung-Chien Chen [a,*], Chiun-Chien Liu [a], Horng-Yuan Jang [b], Pan-Chio Tuan [b]

[a] Department of System Engineering, Chung Cheng Institute of Technology, National Defense University, Tao Yuan 335, Taiwan, ROC
[b] Department of Computer Science & Information Engineering, Nan Kai Institute of Technology, Taiwan, ROC

Received 19 February 2006; received in revised form 11 November 2006
Available online 16 January 2007

Abstract

In this paper, we present an inverse method, an input estimation method, to recursively estimate both the time varied heat flux and the inner wall temperature in the chamber. The algorithm includes the use of the Kalman filter to derive a regression model between the biased residual innovation and the heat flux through a given heat conduction state space model. Based on this regression model, the Recursive Least Squares Estimator (RLSE) is proposed to extract the time-varying heat flux on-line as the input. Computational results show that the proposed method exhibits a good estimation performance and highly facilitates practical implementation.

Keywords: Input estimation method; Heat flux

1. Introduction

Gun barrel heating from multiple firings continues to be a subject of concern to ordnance engineers. Continuous gun firing rises the barrel temperature, producing several adverse effects on system performance. In rapid firing situation, combustion gases and the projectile's sliding friction will produce chemical, mechanical and temperature aspect variation. The propellant gas temperature is the major factor to make gun material melting, cracked, erosion, and wear, etc. [1–4]. An excellent review of gun barrel erosion was given by Ahmad [5]. Ebihara and Rorabaugh [6] describe various erosion mechanisms and Bracuti [7] discusses the role of wear reducing additives. After repeated firings the inner wall temperature increases quickly and reaches the chrome layer melting point. Coating embrittlement by propellant gas product absorption can adversely affect barrel wall resistance to thermal shock and sliding wear [8]. High temperatures will reduce the normal barrel fatigue life.

A number of investigators have modeled barrel heating [9–15]. Some resent publications include: Gerber and Bundy (1991,1992,1993,1995) and Conroy (1991). In these studies, the finite-difference scheme used to solve the problem numerically and described in detail. The reliable gun tube design strongly depends on theoretical analysis and experimental experience. The chamber temperature is related to the barrel material and fire frequency. Thermal effects resulting from high temperature propellant gas and friction action between the bullet band and gun bore result in barrel melting, erosion and wear, thermal stress and deformation, propellant self-ignition or combustion in the cartridge case. These failures lead to reduction in muzzle velocity, range and accuracy, limiting gun performance of guns, and become restrictions to improvements of gun power.

Unknown heat source or heat flux estimation utilizing a measured temperature inside a heat-conducting solid is called the inverse heat conduction problem (IHCP). Inverse heat conduction problems have been of interest to many researchers in recent years. It is sometimes necessary to calculate the transient surface heat flux and the surface temperature from a temperature measured at some location inside a body. The primary heat transfer mechanism to

* Corresponding author. Tel.: +886 3 3809257; fax: +886 3 3906385.
E-mail address: chojan@ccit.edu.tw (T.-C. Chen).

0017-9310/$ - see front matter
doi:10.1016/j.ijheatmasstransfer.2006.11.022

Nomenclature

B	sensitivity matrix	R	measurement noise covariance
$[B]$	gradient matrix	R_o	radius of outer wall
$[C]$	capacitance matrix	R_i	radius of inner wall
C_p	specific heat	s	innovation covariance
C_c	chrome specific heat	t	time
C_s	steel specific heat	T	temperature
$[D]$	matrix of conductivity values	T_0	initial temperature
$\{F\}$	thermal load vector	v	measurement noise vector
$\{ff\}$	coefficient vector	r	radial coordinate
H	measurement matrix	$Z(k)$	observation vector
I	identity matrix	γ	forgetting factor
J	functional	α	thermal diffusivity
J^e	element functional	α_c	thermal diffusivity of the chrome
k	time (discretized)	α_s	thermal diffusivity of the steel
k_c	chrome thermal conductivity	β	impulse duration time
k_s	steel thermal conductivity	Γ	input matrix
K	Kalman gain	δ	Dirac delta function
K_b	steady-state correction gain	ρ	density
l	element length	ρ_c	density of the chrome
M	sensitivity matrix	ρ_s	density of the steel
$[M]$	global conductance matrix	Φ	state transition matrix
N	total number of nodes	Ψ	coefficient matrix
$[N]$	shape function matrix	Ω	coefficient matrix
P	filter's error covariance matrix	Δt	sampling time interval
P_b	error covariance matrix	ω	process noise vector
Q	process noise covariance	σ	standard deviation
$q(t)$	heat flux		

the gun barrel from firing is thermal convection from the propellant gas behind the projectile to the bore surface. The bullet fires within a short time, the propellant gas produces heat flux convection to the wall. In high rate machine gun continuous firing the time interval is very short, allowing the heat flux to accumulate so fast that the inner wall temperature increases sharply. This situation produces heat input from projectile passage mechanisms that can melt the bore surface material.

The time varied heat flux acting on the inner wall is difficult to measure from the inner wall temperature. Therefore, how to estimate the inner wall temperature is very important. If we know the inner wall temperature, better gun material and strength can be designed. This paper concerns the boundary heat flux estimation in a one-dimensional heat conduction domain with heat flux in the chamber wall and convection in the outer wall. The cross-sectional average temperature of the flow in the bore T_g and the coefficient of heat transfer between the gas-particle mixture in the bore and the inner wall of the barrel h_g were obtained from experiments. The T_g and h_g values were difficult to obtain. In this paper, we present an inverse method in which the input estimation method, including a finite-element scheme, is used to solve the estimating time-varying unknown surface heat flux inverse problem. The finite-element discretization concept has been applied to the inverse heat conduction problem [16]. The input estimation method uses the Kalman filter to generate the residual innovation sequence. Based on the regression model, the Recursive Least Squares Estimator (RLSE) is proposed to on-line extract the time-varying heat flux named as the input. The simulation results demonstrate good performance and accuracy in tracking the unknown boundary heat flux of a thermal system. Estimating the unknown heat flux presents a very important reference for understanding the inner wall melting and material phase change necessary to design propellant grain types and barrel materials.

2. The weighting input estimation algorithm

The recursive input estimation algorithm consists of two parts. The first part is a Kalman filter. The second part is a real-time least squares algorithm. The input parameter is the unknown time-varying heat flux. The Kalman filter requires an exact knowledge of the process noise variance Q and the measurement noise variance R, R depends on the sensor measurements. The Kalman filter is used to generate the residual innovation sequence. This recursive real time least-squares algorithm is derived by residual sequence to compute the value of the input heat flux. The actual values derived in the paper [17].

The Kalman filter equations are given by

$$\overline{X}(k/k-1) = \Phi\overline{X}(k-1/k-1) \tag{1}$$

$$P(k/k-1) = \Phi P(k-1/k-1)\Phi^{T} + \Gamma Q\Gamma^{T} \tag{2}$$

$$s(k) = HP(k/k-1)H^{T} + R \tag{3}$$

$$K(k) = P(k/k-1)H^{T}s^{-1}(k) \tag{4}$$

$$P(k/k) = [I - K(k)H]P(k/k-1) \tag{5}$$

$$\overline{Z}(k) = Z(k) - H\overline{X}(k/k-1) \tag{6}$$

$$\overline{X}(k/k) = \overline{X}(k/k-1) + K(k)\overline{Z}(k) \tag{7}$$

The equations for a recursive least-squares algorithm are

$$B(k) = H[\Phi M(k-1) + I]\Gamma \tag{8}$$

$$M(k) = [I - K(k)H][\Phi M(k-1) + I] \tag{9}$$

$$K_{b}(k) = \gamma^{-1}P_{b}(k-1)B^{T}(k)[B(k)\gamma^{-1}P_{b}(k-1)B^{T}(k) + s(k)]^{-1} \tag{10}$$

$$P_{b}(k) = [I - K_{b}(k)\mathrm{B}(k)]\gamma^{-1}P_{b}(k-1) \tag{11}$$

$$\hat{q}(k) = \hat{q}(k-1) + K_{b}(k)[Z(k) - \mathrm{B}(k)\hat{q}(k-1)] \tag{12}$$

where $\hat{q}(k)$ is the estimated input vector, $P_b(k)$ is the error covariance of the estimated input vector, $B(k)$ and $M(k)$ are the sensitivity matrices, and K_b is the Kalman gain. $\overline{Z}(k)$ is the bias innovation caused by measurement noise and input disturbance. $s(k)$ is the covariance of the residual. γ is a forgetting factor.

In this paper, we choice $\gamma = 0.925$ [18] to compromise between fast adaptive capability and the estimate accuracy loss.

3. Mathematical model

Assume that there is a gun barrel is a hollow cylinder. The radii of the inner and outer walls are R_i and R_o, respectively. The radius of the interface between the two metal layers is R_L: and $d_c(\equiv R_L - R_i)$ is the thickness of the chrome layer. The measured temperature $z(t)$ is from the thermocouple at $x = R_o$. Fig. 1 shows the geometry and coordinates. The following restrictions apply here [12]:

(1) The temperature gradients in the axial direction are neglected in comparison to those in the radial direction.
(2) The temperature is axi-symmetrical in the plane normal to the bore axis. This implies axi-symmetrical heat input, as well neglecting gravity in the barrel wall and chrome thickness variation along with other effects that would cause azimuthal dependence.
(3) The barrel feedback heating to the gas flow in the gun bore is neglected.
(4) Barrel thermal expansion is not considered to have an effect on the heat transfer process.
(5) The densities, specific heats, and thermal conductivities of the barrel steel and chrome layer are all constants.

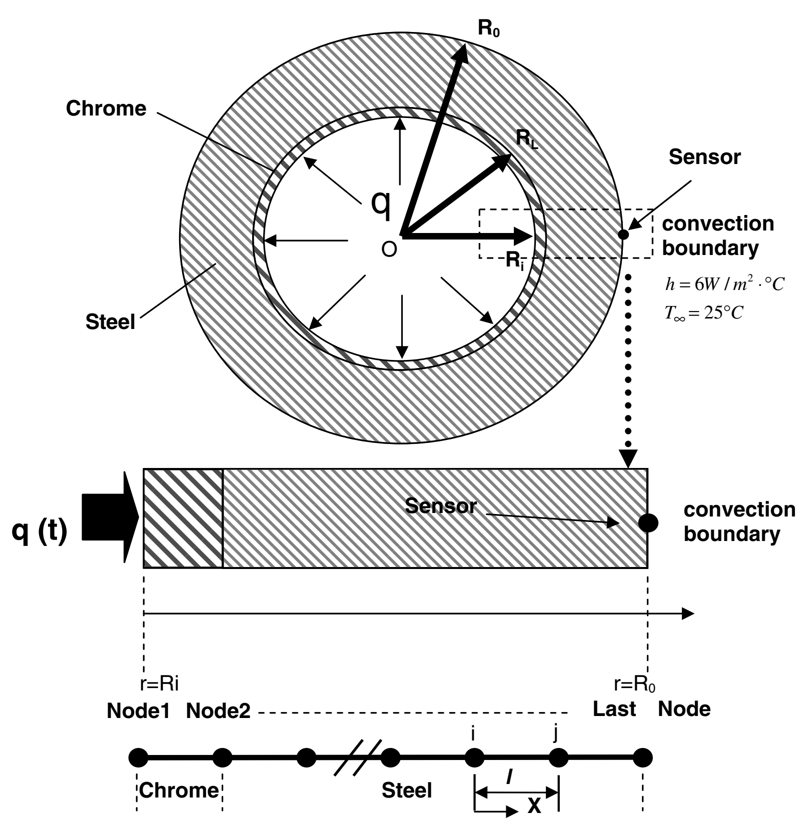

Fig. 1. Geometry and coordinates.

(6) Thermally perfect contact is assumed at the chrome-steel interface (i.e., temperature and radial conductive heat flux are continuous).
(7) The latent heat effects due to phase change in the steel from martensite to austenite are neglected.

The mathematical formulation of the one-dimensional, transient, heat conduction problem can be generalized as:

$$\frac{\partial^2 T(r,t)}{\partial r^2}+\frac{1}{r}\frac{\partial T(r,t)}{\partial r}=\left(\frac{1}{\alpha_c}\right)\frac{\partial T(r,t)}{\partial t} \quad \text{in } R_i \leqslant r \leqslant R_L, \tag{13}$$

and

$$\frac{\partial^2 T(r,t)}{\partial r^2}+\frac{1}{r}\frac{\partial T(r,t)}{\partial r}=\left(\frac{1}{\alpha_s}\right)\frac{\partial T(r,t)}{\partial t} \quad \text{in } R_L \leqslant r \leqslant R_o, \tag{14}$$

$$T(r,0)=T_0 \quad \text{for } t=0, \quad \text{in } R_i \leqslant r \leqslant R_o \tag{15}$$

$$-k_c\frac{\partial T}{\partial r}=q(t) \quad \text{in } r=R_i, \tag{16}$$

$$-k_s\frac{\partial T}{\partial r}=h(T-T_\infty) \quad \text{in } r=R_o, \tag{17}$$

$$k_c\left(\frac{\partial T}{\partial r}\right)_c=k_s\left(\frac{\partial T}{\partial r}\right)_s \quad \text{in } r=R_L, \tag{18}$$

$$Z(r,t)=T(r,t)+v(t) \quad \text{measured temperature} \tag{19}$$

where T is the temperature distribution as is function of r and t, $t=$ time measured from firing initiation. The constants $\alpha_c \equiv k_c/(\rho_c \cdot c_{p_c})$ and $\alpha_s \equiv k_s/(\rho_s \cdot c_{p_s})$ are the thermal diffusivities of the chrome and steel, respectively. Here k_c,ρ_c and c_{p_c} are the thermal conductivity, density, and specific heat, respectively of the chrome; k_s, ρ_s and c_{p_s} are the corresponding properties of the steel.

Where T_0 is the uniform initial temperature, $q(t)$ is the unknown heat flux input to be estimated, and $Z(t)$ is the noise-corrupted measurement, $v(t)$ is the measurement noise assumed zero mean and white Gaussian, h is the coefficient of convective heat transfer between the barrel wall and the surrounding atmosphere, T_∞ is outer wall temperature.

In chrome layer $R_i \leqslant r \leqslant R_L$, The calculus of variations provides an alternative method for formulating the governing Eq. (13) and boundary conditions (15), (16), and (18). Variational calculus states that the minimization of the functional J_c [19]:

$$J_c=\frac{1}{2}\int\int_V\int\left[rk_c\cdot\left(\frac{\partial T}{\partial r}\right)^2+2r\rho_c C_c\cdot\left(\frac{\partial T}{\partial t}\right)\cdot T\right]dV + \int_S qT\,dS \tag{20}$$

The element equation for the temperature is $T^e=N_i^eT_i+N_j^eT_j=[N^e]\{T\}$where T_i and T_j are the nodal temperatures to be determined.

$$[N^e]=[N_i^e\ N_j^e]=\left[\frac{R_j-r}{R_j-R_i}\ \frac{r-R_i}{R_j-R_i}\right]$$

the temperature gradient matrix $\{g^e\}$, is given by

$$\{g^e\}=\frac{\partial T^e}{\partial r}=\left[\frac{\partial N_i^e}{\partial r}\ \frac{\partial N_j^e}{\partial r}\right]\{T\}=-\frac{1}{R_j-R_i}T_i+\frac{1}{R_j-R_i}T_j = \left[-\frac{1}{R_j-R_i}\ \ \frac{1}{R_j-R_i}\right]\left\{\begin{matrix}T_i\\T_j\end{matrix}\right\}=[B^e]\{T\}$$

where $[N]$ is the shape function matrix, $[B]$ is obtained by differentiating $[N]$ with respect to r.

Eq. (20) must be minimized with respect to the set of nodal values $\{T\}$

$$\frac{\partial J_c}{\partial\{T\}}=\frac{\partial}{\partial\{T\}}\sum_{e=1}^{E}J_c^e=\sum_{e=1}^{E}\frac{\partial J_c^e}{\partial\{T\}}=0$$

The minimization process produces the following system of equations.

$$[C]_c\frac{\partial\{T\}}{\partial t}+[M]_c\{T\}+\{F\}_c=0$$

The $[C]_c$ matrix is the global capacitance matrix, $[M]_c$ is the global conductance matrix, $\{F\}_c$ is the thermal load vector. The element contributions to $[C]_c$, $[M]_c$, $\{F\}_c$ are summed in the usual manner.

$$[D^e]_c=[rk_c^e] \tag{21}$$

$$[C^e]_c=\int_V r\rho_c C_c[N^e]\{T\}[N^e]\frac{\partial\{T\}}{\partial t}dV=\frac{2\pi\rho_c C_c}{60l^2}\begin{bmatrix}(2R_j^5-20R_j^2R_i^3+30R_jR_i^4-12R_i^5) & (3R_j^5-5R_j^4R_i+5R_jR_i^4-3R_i^5)\\(3R_j^5-5R_j^4R_i+5R_jR_i^4-3R_i^5) & (12R_j^5-30R_j^4R_i+20R_j^3R_i^2-2R_i^5)\end{bmatrix} \tag{22}$$

$$[M^e]_c=\int_V[B^e]^T[D^e]_c[B^e]dV = \frac{2\pi k_c}{l^2}\int_{R_i}^{R_j}\begin{bmatrix}-1\\1\end{bmatrix}[-1\quad 1]r^2\,dr=\frac{2\pi k_c(R_j^3-R_i^3)}{3(R_j-R_i)^2}\begin{bmatrix}1 & -1\\-1 & 1\end{bmatrix} \tag{23}$$

$$\{f^e\}_c=\int_{S_1}q[N^e]^T dS=\{ff\}q=2\pi R_i q\begin{bmatrix}1\\0\end{bmatrix} \tag{24}$$

where R_i, R_j are the single element left node and right node. $l=R_j-R_i$ is the length of single element. $[D]$ is matrix consists of the conductivity values. $[ff]$ is the coefficient matrix.

In the steel layer, The functional formulation that is equivalent to (14) and its boundary conditions (15), (17) and (18) is J_s:

$$J_s=\frac{1}{2}\int\int_V\int\left[rk_s\cdot\left(\frac{\partial T}{\partial r}\right)^2+2r\rho_s C_s\cdot\left(\frac{\partial T}{\partial t}\right)\cdot T\right]dV + \int_{S_1}\frac{1}{2}h(T-T_\infty)^2 dS \tag{25}$$

$$J=\sum_{e=1}^{E}\int_{V^e}\frac{1}{2}\{g^e\}^T[D^e]\{g^e\}dV+\int_V r(\rho_s C_s)^e\left(\frac{\partial T^e}{\partial t}\right)T^e dV + \int_{S_1^e}\frac{1}{2}h(T^e-T_\infty^e)^2 dS \tag{26}$$

We take a single element

$$J_s^e = \int_{V^e} \frac{1}{2}\{T\}^T\{B^e\}^T[D^e]\{B^e\}\{T\}dV + \int_{V^e} r\rho_s C_s[N^e]\{T\}[N^e]\frac{\partial\{T\}}{\partial t}dV + \int_{S_1^e} \frac{h}{2}\{T\}^T\{N^e\}^T\{N^e\}\{T\}dS - \int_{S_1^e} hT_\infty\{N^e\}\{T\}dS + \int_{S_1^e}\frac{h}{2}hT_\infty^2\,dS \quad (27)$$

In the steel layer, Eq. (27) must be minimized with respect to the set of nodal values $\{T\}$:

$$\frac{\partial J_s}{\partial\{T\}} = \frac{\partial}{\partial\{T\}}\sum_{e=1}^{E} J_s^e = \sum_{e=1}^{E}\frac{\partial J_s^e}{\partial\{T\}} = 0$$

We can get steel layer single element matrix $[C^e]_s$, $[M^e]_s$, $\{f^e\}_s$, respective:

$$[D^e]_s = [rk_s^e] \quad (28)$$

$$[C^e]_s = \int_V r\rho_s C_s[N^e]\{T\}[N^e]\frac{\partial T}{\partial t}dV = \frac{2\pi\rho_s C_s}{60l^2}\begin{bmatrix}(2R_j^5 - 20R_j^2R_i^3 + 30R_jR_i^4 - 12R_i^5) & (3R_j^5 - 5R_j^4R_i + 5R_jR_i^4 - 3R_i^5)\\ (3R_j^5 - 5R_j^4R_i + 5R_jR_i^4 - 3R_i^5) & (12R_j^5 - 30R_j^4R_i + 20R_j^3R_i^2 - 2R_i^5)\end{bmatrix} \quad (29)$$

$$[M^e]_s^1 = \int_V [B^e]^T[D^e]_s[B^e]dV = \frac{2\pi k_s}{l^2}\int_{R_i}^{R_j}\begin{bmatrix}-1\\1\end{bmatrix}[-1 \quad 1]r^2\,dr = \frac{2\pi k_s(R_j^3 - R_i^3)}{3(R_j - R_i)^2}\begin{bmatrix}1 & -1\\ -1 & 1\end{bmatrix} \quad (30)$$

In the right node ($N_i = 0$, $N_j = 1$, $r = R_j$)

$$[M^e]_s^2 = \int_{S_2^e} h\{N^e\}^T\{N^e\}dS = \int_{S_2^e} h\begin{bmatrix}N_iN_i & N_jN_i\\ N_iN_j & N_jN_j\end{bmatrix}dS = 2\pi R_o h\begin{bmatrix}0 & 0\\ 0 & 1\end{bmatrix}$$

Merging $[M^e]_s^1$ *ms* for element $1, 2, \ldots, n$ and $[M^e]_s^2$.

$$[M^e]_s = [M^e]_s^1 + [M^e]_s^2 = \begin{bmatrix} m_1 & -m_1 & 0 & 0 & 0 & 0\\ -m_1 & m_1+m_2 & -m_2 & 0 & 0 & 0\\ 0 & -m_2 & m_2+m_3 & -m_3 & 0 & 0\\ 0 & 0 & -m_3 & m_3+m_4 & \cdots & \cdots\\ \cdots & \cdots & \cdots & \cdots & \ddots & -m_n\\ 0 & 0 & 0 & 0 & -m_n & m_n + 2\pi R_o h\end{bmatrix} \quad (31)$$

$$\{f^e\}_c = \int_{S_1^e} hT_\infty\{N^e\}^T dS = \int_{S_1^e} hT_\infty\begin{bmatrix}0\\1\end{bmatrix}dS = 2\pi R_o \cdot hT_\infty\begin{bmatrix}0\\1\end{bmatrix} \quad (32)$$

Assemble the chrome layer and steel layer element, then minimized with respect to the set of nodal values $\{T\}$:

$$\frac{\partial J}{\partial\{T\}} = \frac{\partial}{\partial\{T\}}\sum_{e=1}^{E} J^e = \sum_{e=1}^{E}\frac{\partial J^e}{\partial\{T\}} = 0 \quad (33)$$

where Eq. (33) is a system of first-order linear differential equations.

$$[C]\frac{\partial\{T\}}{\partial t} + [M]\{T\} + \{F\} = 0 \quad (34)$$

The $[C]$ matrix is the capacitance matrix, $[M]$ is the conductance matrix, $\{F\}$ is the thermal load vector. From Eq. (34) and to account for process noise inputs [20], the continuous time state equation can be written as:

$$\dot{T}(t) = \Psi T(t) + \Omega[q(t) + w(t)] \quad (35)$$

$$\Psi = (-1)[C]^{-1}[M], \quad \Omega = (-1)[C]^{-1}\{ff\}$$

where the state vector $T(t)$ is $N \times 1$, N is the total nodes, Ψ and Ω are the coefficient matrix. Ψ is $N \times N$, Ω is $N \times 1$, q is the unknown input heat flux of the boundary, $\omega(t)$ is the process noise. This noise term represents the modeling error. We replace the time derivative with a forward difference, discrete over time intervals of length Δt is

$$X(k) = \Phi X(k-1) + \Gamma[q(k-1) + \omega(k-1)] \quad (36)$$

where

$$X(k-1) = [T_1 \quad T_2 \quad T_3 \ldots \quad T_{N-1} \quad T_N]^T,$$

$$\Phi = e^{\Psi\Delta t}$$

$$\Gamma = \int_{k\Delta t}^{(k+1)\Delta t}\exp\{\Psi[(k+1)\Delta t - \tau]\}\Omega\,d\tau$$

Here X represent the state vector, Φ is the state transition matrix, Γ is the input matrix, q is the deterministic input sequence and ω is the process noise vector, assumed to be zero mean and white noise with variance

$$E\{\omega(k)\omega^T(j)\} = Q\delta_{kj}$$

where δ_{kj} is a Dirac delta function. In order to compare the results for situations involving measurement errors, using Eq. (19), the discrete measure equation becomes:

$$Z(k) = HX(k) + v(k) \quad (37)$$

where Z is the observation vector at time $k\Delta\tau$, H is the measurement matrix, v is the measurement noise vector, assumed to be zero mean and white. The variance of $v(k)$ is given by $E\{v(k)v^T(j)\} = R\delta_{kj}$.

The obtained state equation is combined with the Kalman filter and recursive least squares method to progress the inverse estimation.

4. Results and discussion

Using simulation, a 5.56 mm T65K2 rifle three-shot and 5.56 mm machine gun under continuous fire situations were modeled. The thermal and mechanical properties of the gun steel (AISI 4340) and its associated chrome layer were taken as [12]:

Specific heat, $C_s = 469.05$ J/(kg °C), $C_c = 505.03$ J/(kg °C)
Density, $\rho_s = 7827$ kg/m^3, $\rho_c = 7191$kg/m^3
Thermal conductivity, $k_s = 38.07$ J/(m s °C), $k_c = 83.75$ J/(m s °C)

Thermal diffusivity, $\alpha_s = 1.037 \times 10^{-5}\ \mathrm{m^2/s}$, $\alpha_c = 2.305 \times 10^{-5}\ \mathrm{m^2/s}$

Melting temperature $(T_m)_s = 1504\ ^\circ\mathrm{C}$, $(T_m)_c = 1857\ ^\circ\mathrm{C}$

Here we consider two gun barrels, a T65K2 rifle barrel, and a 5.56 mm machine gun barrel

T65K2 rifle, ($R_i = 0.00278$ m and $R_o = 0.00720$ m)

5.56 mm machine gun ($R_i = 0.00278$ m and $R_o = 0.00828$ m).

To illustrate the accuracy of the proposed approach in predicting input heat flux $\hat{q}(k)$, we used a representative one dimension unknown triangle wave heat flux to check the feasibility of the weighting input estimation method combined finite element method. A thermocouple was placed at the surface $x = R_o$, the coefficient of convective heat transfer between the barrel wall and the surrounding atmosphere $h = 6\ \mathrm{W/m^2\ ^\circ C}$ [12], $T_\infty = 25\ ^\circ\mathrm{C}$ is outer wall temperature. Since $P(-1/-1)$ and $P_b\,(-1)$ are normally not known, the estimator was initialized with $P(-1/-1)$ and $P_b\,(-1)$ as very large numbers, such as 10^8, respectively. This had the effect of treating the initial errors as very large, so the estimator ignored the first few initial estimates. The initial input estimator CONDITIONS were given by $\overline{X}(-1/-1) = [0 \quad 0 \quad \ldots \quad 0]^T$ and $P(-1/-1) = \mathrm{diag}[10^8]$ for the Kalman filter. The real-time least-squares algorithm initial conditions were given by $\hat{q}(-1) = 0, P_b(-1) = 10^8$ and $M(-1)$ was set using a zero matrix. The Kalman filter for the recursive input estimation algorithm requires exact knowledge of the process noise covariance matrix Q and the measurement noise covariance matrix R. R depends on the sensor measurements. Both the filter Q value and sequential least-square γ value interactively affect the fast adaptive capability for tracking the time-varying parameter. The test input heat flux is given by

Example 1. Triangle waveform in $q(t)\,(\mathrm{W/m^2})$

$$q(t) = \begin{cases} 0 & 0 \leqslant t < 4, \quad 10 < t \leqslant t_f \\ 10^6 \times (0.25t - 1) & 4 \leqslant t \leqslant 8 \\ 10^6 \times (-0.5t + 5) & 8 \leqslant t \leqslant 10 \end{cases} \tag{38}$$

The sampling interval $\Delta t = 0.01$ s, the estimation input heat flux $q(t)$ on the boundary $x = R_i$, at $x = R_o$ is convection situation $h = 6\ \mathrm{W/m^2\ ^\circ C}$, $T_\infty = 25\ ^\circ\mathrm{C}$, the sensor location is at $x = R_o$, the element number $E = 550$, the initial temperature $T_0 = 0\ ^\circ\mathrm{C}$, process noise covariance $Q = 10$, and measurement noise covariance $\sigma = 10^{-4}$, $\sigma = 10^{-3}$. The estimates of $q(t)$ are plotted in Fig. 2 for $\sigma = 10^{-4}$ and $\sigma = 10^{-3}$, respectively. This indicates that a large measurement error can cause estimate accuracy degradation. In this case, although the measurement error influences the estimate resolution, the results are still good.

Example 2. Square waveform in $q(t)\,(\mathrm{W/m^2})$

$$q(t) = \begin{cases} 0 & 0 \leqslant t < 2, \quad 27 < t \leqslant t_f \\ 7 \times 10^5 & 2 \leqslant t \leqslant 27 \end{cases} \tag{39}$$

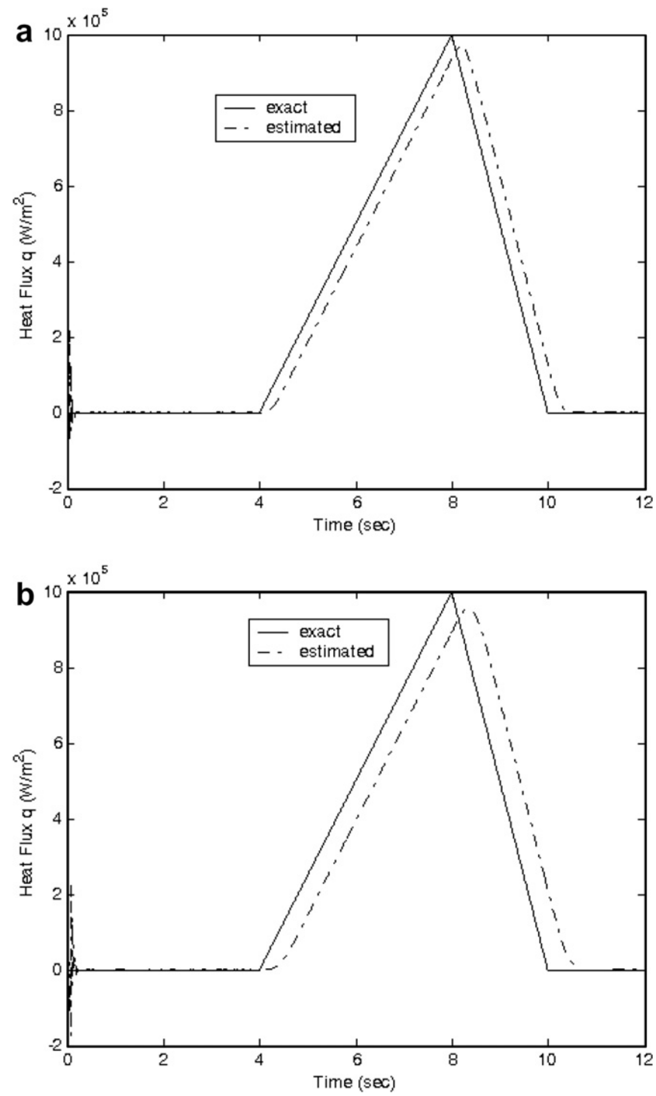

Fig. 2. (a) Estimated triangle wave as input heat flux with $\sigma = 10^{-4}$, $Q = 10$. (b) Estimated triangle wave as input heat flux with $\sigma = 10^{-3}$, $Q = 10$.

We used the following test condition and parameters: 5.56 mm machine gun, continuous fire at 25 s, if we assume the heat flux become reduce the firing time can be prolong, the round-for-round time was very short and neglected, the sampling interval $\Delta t = 0.01$ s, elements number $E = 550$, process noise covariance $Q = 10$, and measurement noise covariance $\sigma = 10^{-4}$, $\sigma = 10^{-3}$. Figs. 3 and 4 demonstrate the temperature figure. The estimates of $q(t)$ are plotted in Fig. 5 for $\sigma = 10^{-4}$ and $\sigma = 10^{-3}$, respectively. From Fig. 3a we can find the chrome layer melting point at 1857 °C. Under continuous fire the melting point will be reached in about 22 s. From Fig. 5 it is evident that the recovery of $q(t)$ using the weighting input estimation method combined with the finite element method is good. The estimation results show excellent agreement with the exact value. Using this method, we can use the measured temperature to recursively estimate both the time varied heat flux in the chamber and the inner wall temperature.

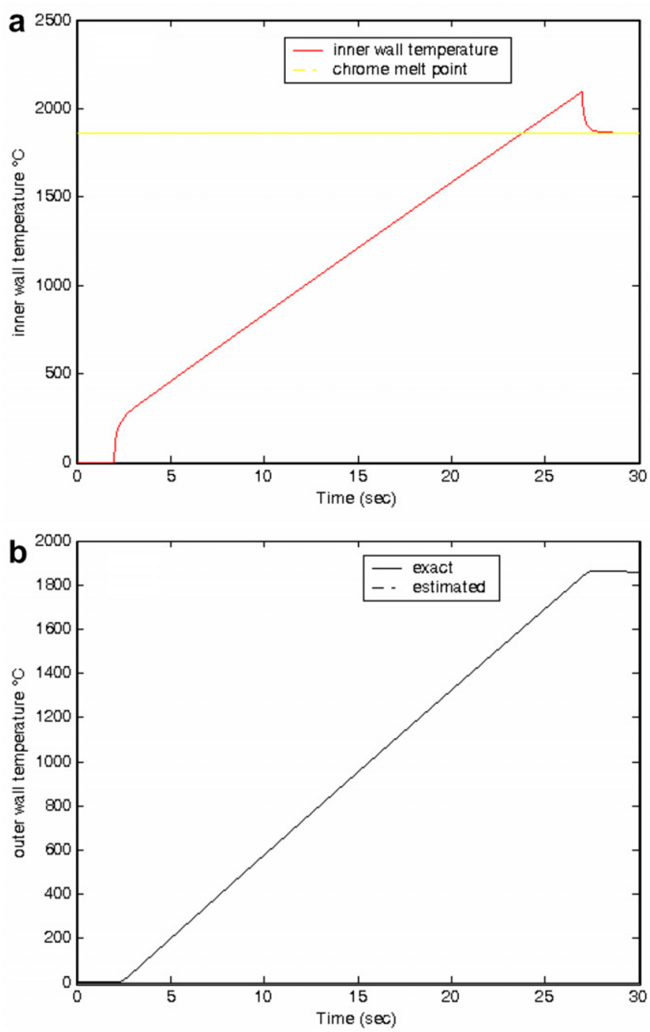

Fig. 3. (a) Continuous fire inner wall temperature. (b) Continuous fire outer wall temperature.

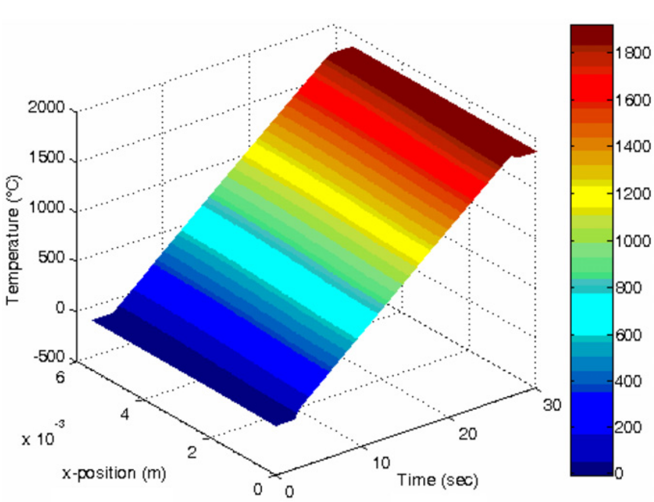

Fig. 4. Continuous fire 3D temperature.

The proposed scheme is helpful in developing future nondestructive experiments. The temperature influence on

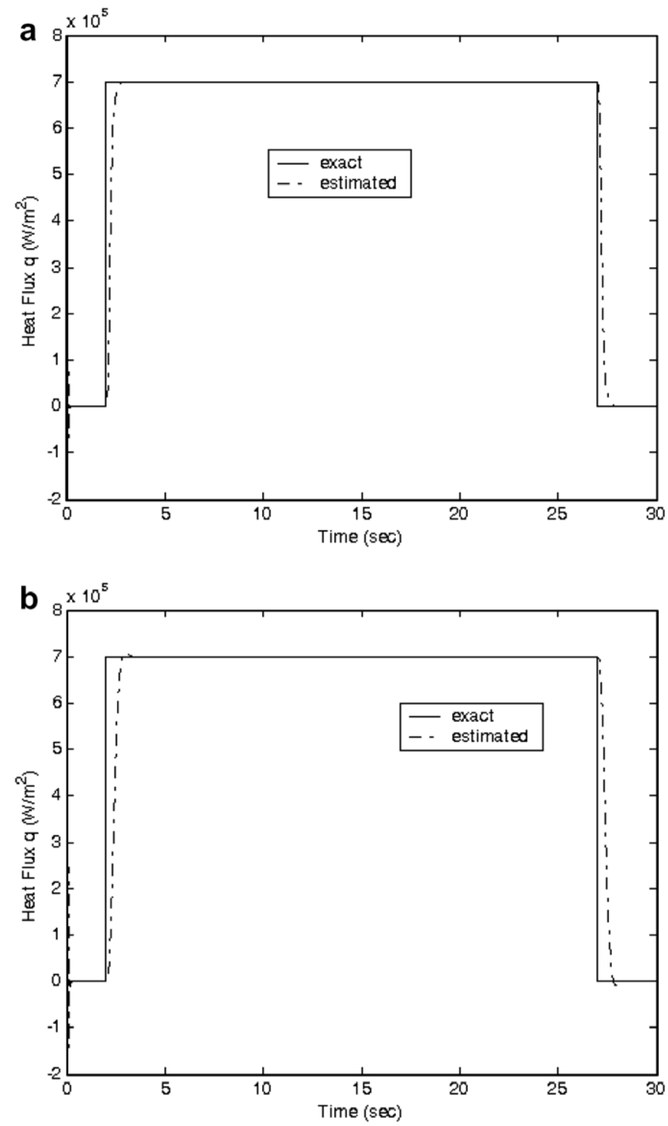

Fig. 5. (a) Estimated continuous fire with $\sigma = 10^{-4}$, $Q = 10$. (b) Estimated continuous fire with $\sigma = 10^{-3}$, $Q = 10$.

a shooter, gun material and propellant testing are fast and economical. These applications can be useful in making quick and efficient identification of unknown heat flux in the chamber surface.

Example 3. Three-shot square waveform in $q(t)\,(\mathrm{W/m^2})$

$$q(t) = \begin{cases} 7 \times 10^5 & 1 \leqslant t \leqslant 1.3, \quad 1.4 \leqslant t \leqslant 1.7, \\ & 1.8 \leqslant t \leqslant 2.1, \quad 2.2 \leqslant t \leqslant 2.5 \\ & 2.6 \leqslant t \leqslant 2.9, \quad 3.0 \leqslant t \leqslant 3.3 \\ 0 & \text{others} \end{cases} \tag{40}$$

The following test condition and parameters: 5.56 mm TK65K2 rifle gun, three-shot six times, round-for-round time was very short and neglected, sampling interval $\Delta t = 0.001$ s, elements number $E = 450$, process noise covariance $Q = 10$, and measurement noise covariance $\sigma = 10^{-4}$. The estimates of $q(t)$ are plotted in Fig. 6a. It was found that Fig. 6a shows larger fluctuations in the esti-

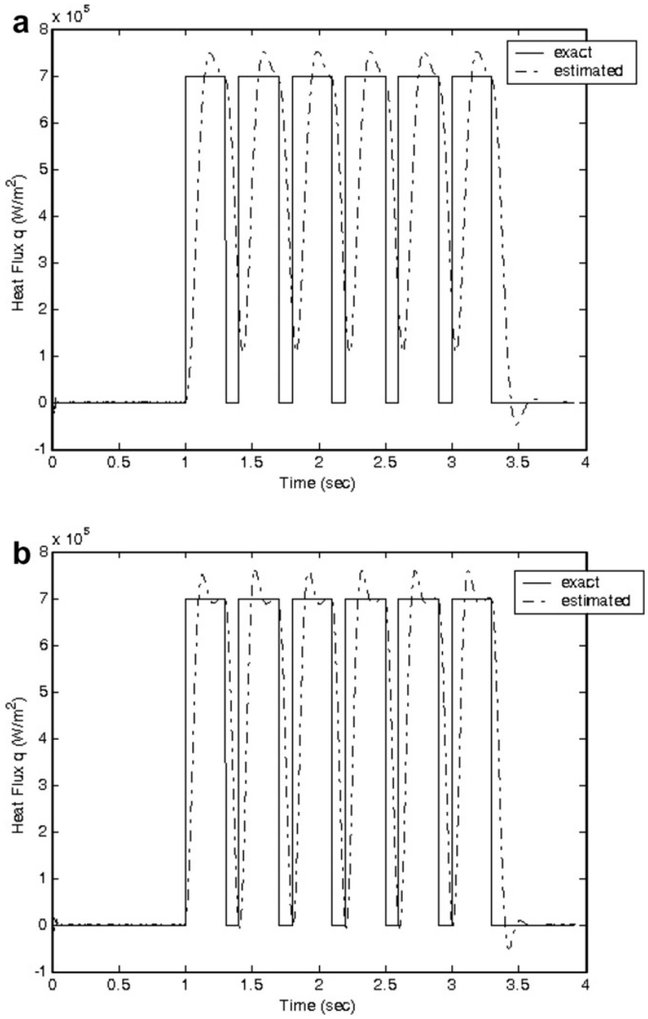

Fig. 6. (a) Estimated three-shot fire with $\sigma = 10^{-4}$, $Q = 10$. (b) Estimated three-shot fire with $\sigma = 10^{-4}$, $Q = 100$.

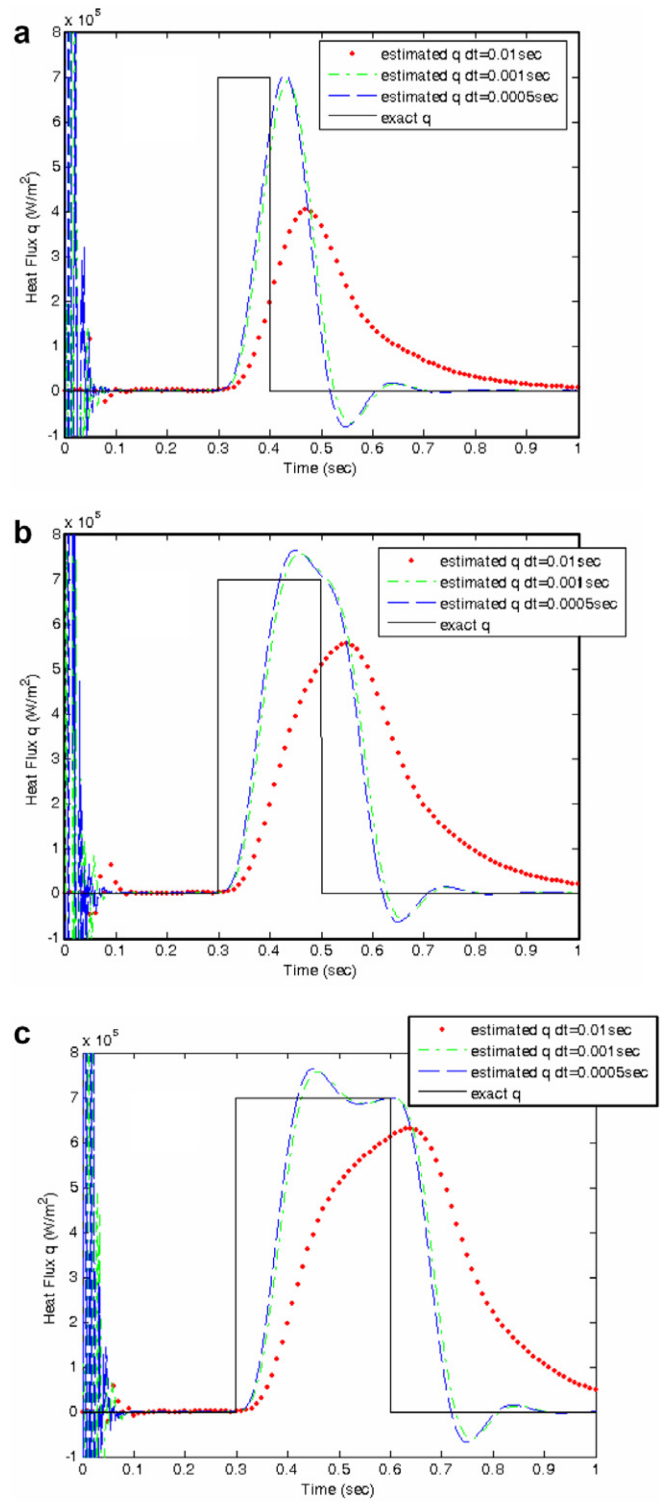

Fig. 7. (a) Comparison between the estimated $\beta = 0.1$ s with $\Delta t = 0.01$, 0.001, 0.0005 s. (b) Comparison between the estimated $\beta = 0.2$ s with $\Delta t = 0.01$, 0.001, 0.0005 s. (c) Comparison between the estimated $\beta = 0.3$ s with $\Delta t = 0.01$, 0.001, 0.0005 s.

mated value than Fig. 5. This indicates that fast pulse heat flux can cause estimate accuracy degradation. In Fig. 6b, $Q = 100$ the estimates of $q(t)$ were better than those in Fig. 6a. In this case, although the fast pulse heat flux influences the estimate resolution, the results are still acceptable.

In order to analyze the influences in estimation results produced by using different impulse duration and sampling time, the results of tests are shown in Fig. 7. The three sets of sampling time, $\Delta t = 0.01$, 0.001, and 0.0005 s, and the three sets of impulse duration time, $\beta = 0.1$, 0.2, and 0.3 s. According to the figure, the estimation is precise for different impulse duration when the sampling time (Δt) is 0.001 s. The estimation has slightly better result when $\Delta t = 0.0005$ s. However, the improvement is not significant. As a result, when Δt is shorter than 0.0005 s, the computing time in the simulation will be longer. The results of estimation may not even converge due to the relatively greater influence of noise than the change of temperature in a very short time interval.

The above simulation results demonstrates that the proposed method has good performance in tracking unknown heat flux imposed on a gun barrel wall in a one-dimensional body.

5. Conclusions

This research used simulations of the measured temperature on a gun barrel outer wall to estimate the heat flux in the chamber on-line with accuracy. The measurement data can be used to understand all temperature fields. We found that the heat flux input from projectile passage mechanisms can melt/erode the bore surface material. If we know the temperature variability, we can then avoid reaching the gun material melting point. The proposed scheme is helpful in developing future nondestructive experiments and design propellant grain types and barrel materials. The time varied heat flux of a gun barrel was estimated precisely on-line in this study. The total temperature field inside the gun barrel was estimated to determine the gun material melting point using the temperature variation. This kind of nondestructive experiment can provide fast economical gun barrel and propellant research. The heat pulse flux produced by the bullet occurs simultaneously after shooting from the barrel in continuous shooting cases. Therefore, the proposed method is sensitive to the temperature delay effect and measurement accounting. We must choose a large Q and to acquire better estimated results.

Further, systematic study can focus on how to avert the temperature effect on the gun barrel inner wall, determining methods to control heat, such as tantalum or improved chromium coatings to prolong barrel life and reduce maintenance costs. The temperature influence on a shooter, gun material and propellant testing can be determined economically and quickly. These applications can be useful in making quick and efficient identification of unknown heat flux on the chamber surface. The conclusions obtained are valuable in improving the service life of gun barrels and offer a scientific basis for the rational and effective choice of materials.

Acknowledgement

This work was supported by the National Science Council of the Republic of China under Grant NSC93-2212-E-014-009.

References

[1] J. Richard Ward, Timothy L. Brosseau, Bertram B. Grollman. Heat Transfer in Guns-Determination of Friction Factor From Heat Input Measurements (ADA105430), U.S. Army Armament Research and Development Command, U.S. Army Ballistic Research Laboratory, Aberdeen Proving Ground, MD, September, 1981.

[2] R.M. Fisher, A. Szirmae, W.T. Huang, Paul J. Conroy. Metallographic Studies of Erosion and Thermo-Chemical Cracking of Cannon Tubes (ADA135816), U.S. Army Armament Research & Development Command Benet Weapons Laboratory, DRDAR-LCB-TL Watervliet, NY 12189, May, 1983.

[3] James N. Blecker. Small Arms Gun Barrel Thermal Experimental Correlation Studies (AD786509), Research Directorate, SARRI-LR GEN Thomas J. Rodman Laboratory Rock Island Arsenal, Rock Island, IL 61201, June, 1974.

[4] Leonard H. Caveny. Steel Erosion Produced by Double Base, Triple Base, and RDX Composite Propellants of Various Flame Temperature, (ADA092344), U.S. Army Armament Research and Development Command, Large Caliber Weapon Systems Laboratory, Dover, New Jersey, October, 1980.

[5] I. Ahmad, in: L. Steifel (Ed.), Gun Propulsion Technology, Progress in Astronautics and Aeronautics, vol. 109, AIAA, Washington, 1988, pp. 311–356.

[6] W.T. Ebihara, D.T. Rorabaugh, in: L. Steifel (Ed.), Gun Propulsion Technology, Progress in Astronautics and Aeronautics, vol. 109, AIAA, Washington, 1988, pp. 357–376.

[7] A.J. Bracuti, in: L. Steifel (Ed.), Gun Propulsion Technology, Progress in Astronautics and Aeronautics, vol. 109, AIAA, Washington, 1988, pp. 377–412.

[8] P.J. Cote, Gas-metal reaction products in the erosion of chromium-plated gun bores, Wear (241) (2000) 17–25.

[9] N. Gerber, M. Bundy, Heating of a Tank Gun Barrel: Numerical Study. BRL-TR-3932 (ADA241136), U.S. Army Ballistic Research Laboratory, Aberdeen Proving Ground, MD, August, 1991.

[10] N. Gerber, M. Bundy. Effect of Variable Thermal Properties on Gun Tube Heating. BRL-TR-3984 (ADA253066), U.S. Army Ballistic Research Laboratory, Aberdeen Proving Ground, MD, July, 1992.

[11] N. Gerber, M. Bundy, Cross-Barrel Temperature Difference Due to Wall Thickness Variation, ARL-TR-100 (ADA262509), U.S. Army Ballistic Research Laboratory, Aberdeen Proving Ground, MD, March, 1993.

[12] N. Gerber, M.L. Bundy, Gun Barrel Heating With Heat Input During Projectile Passage, Journal of Ballistics 12 (4) (1995) 267–281.

[13] Paul J. Conroy, Gun Tube Heating. BRL-TR-3300 (ADA243265), U.S. Army Ballistic Research Laboratory, Aberdeen Proving Ground, MD, December, 1991.

[14] Tony W.H. Sheu, S.H. Lee, Numerical Study of Two-Dimensional Solid–Gas Combustion Through Granulated Propellants, Numerical Heat Transfer, Part A 27 (1995) 395–415.

[15] J.K. Clutter, W. Shyy, Computation of High-Speed Reacting Flow for Gun Propulsion Applications, Numerical Heat Transfer, Part A 31 (1997) 355–374.

[16] T.C. Chen, H.Y. Jang, P.C. Tuan, Input Estimation Method Combining the Finite-Element Scheme for Inverse Heat Flux Estimation in a Barrel Inner Wall, Journal of Explosives and Propellants (2004).

[17] P.C. Tuan, L.W. Fong, W.T. Huang, Analysis of On-Line Inverse Heat Conduction Problems, Journal of Chung Chen Institute of Technology 25 (1) (1996) 59–73.

[18] P.C. Tuan, L.W. Fong, W.T. Huang, Application of Kalman Filtering with input estimation technique to on-line cylindrical inverse heat conduction problems, JSME International Journal, Series B 40 (1) (1997) 126–133.

[19] J.N. Reddy, Applied Functional Analysis and Variational in Engineering, Malabar, Florida, 1991.

[20] A.H. Jazwinski, Stochastic Processes and Filtering Theory, Academic Press, New York, 1970.